recently[10-12] and it has been shown that a silicon thermistor may be used as an X-ray spectrometer[11].

The traditional use of low-temperature bolometers is for the detection of a continuous flux of infrared radiation[13-18]. The instruments based on semiconductors were found to have better performance and to be simpler to use than those based on superconductivity. The semiconductors (doped Ge or Si) have a resistance varying as T^{-4}-T^{-9} in the temperature region of 0.3-5 K. In the early 1970s a new type of bolometer, a so-called composite one, was developed at LPSP[1,14], consisting of an absorber with a large surface area (0.5-20-mm diameter) coupled thermally to a monolithic semiconductor thermistor with very small volume (typically, 0.008 mm^3). Its best performance has been obtained with a diamond wafer as the absorber and a germanium crystal as thermometer. (The use of diamond is especially advantageous because of its very high thermal diffusivity[1].) A schematic diagram of a composite bolometer is shown as an inset in Fig. 1. An asset of this construction is that there is no need for soldering, which results in a minimum of low frequency noise and a low heat capacity.

The essential advantage of the composite bolometer is that it separates the absorbing and detecting functions. The absorber (diamond, sapphire, dielectric-metal sandwich) may be optimized independently of the thermometer, which in turn has to have maximal temperature derivative of the impedance, dZ/dT, and the impedance, Z, matched to the preamplifiers[18]. The use of bolometers for detection of different kinds of flux is increasing steadily: for molecular beams[19,20], for radiation in the millimetre wave-length range[14-18] and, most recently, for X rays[11]. It is also interesting to note that spurious pulses, caused by cosmic-ray absorption in the infrared low-temperature detectors, were deliberately eliminated, using a 'spike suppression circuit', by high-altitude astronomers[21].

The diamond wafer, which acts as the absorber in our bolometer, has a volume 0.25 mm^3. At our working temperature (1.3 K) we have measured the thermalization time of the device to be <60 μs from any point of impact on its surface. The thermometer, which has a surface area of 0.1×0.1 mm^2, is glued to the diamond with a 10-μm layer of epoxy, which eliminates the possibility of charge collection, as there is no bias across the absorber.

The resolution of the detector is only limited by the noise of the detector itself (Johnson noise and thermodynamic noise)(see refs 10 and 18 for a detailed analysis of these noise effects). With optimal filtering, an order of magnitude estimate for the resolution is given by $\Delta U_{FWHM} = a\sqrt{8\,(\ln 2) k_B T^2 C}$ where k_B is the Boltzmann constant, T the temperature of the helium bath (in K) and C the specific heat of the bolometer at the temperature T. The constant a depends on the details of the construction of the bolometer (on dZ/dT and Z) and generally has a value of 1-2; here, $a = 1.5 \pm 0.2$. The limiting resolution calculated from this expression is shown in Fig. 1.

The bolometer used in this experiment is mounted in the vacuum chamber of a commercial portable optical cryostat[22]. A mixed ^{239}Pu, ^{241}Am, ^{244}Cm α source was positioned in front of the diamond so that no particles could reach the Ge thermometer. A Pb shutter could be inserted between source and detector during background measurements. A typical α spectrum measured at a temperature of 1.3 K is shown in Fig. 2. The low-noise preamplifier had a band pass filter of 2-120 kHz and a gain of 2,000 (ref. 23). A 5.5-MeV α particle gives a typical temperature increase of 1 mK. The resolution is 36 keV, which is not yet the best possible performance of the system. The main reason for this is that we have used standard nuclear electronics which could not be optimally matched to the time constant of the bolometer. We are presently working on improvements to both the electronics and the cryostat and hope soon to have an operational α detector with a resolution of ~3 keV at 1 K. We foresee that the technique of nuclear radiation detection via thermal pulses will have a great impact on many fields of physics.

H.H.S. thanks the NSF for support through grant no. PHY 8204402.

Received 3 December 1984; accepted 10 January 1985.

1. Leblanc, J., Dambier, G., Coron, N. & Moalic, J. P. *French Patents* No.75 36103 and 75 36104 (26 Nov. 1975) and *US Patent* No. 4, 116, 063 26 (Sept. 1978).
2. De Rújula, A. *Nucl. Phys.* B188, 414-458 (1981).
3. Laegsgaard, E. *et al.* in *Proc. 7th Int. Conf. Atomic Masses and Fundamental Constants* (AMCO-7) (ed. Klepper, O.) 652-658 (TDH-Schrittenreihe Wissenschaft und Technik, Darmstadt, 1984).
4. De Rújula,A. & Lusignoli, M. *Phys. Lett.* 118B, 429-434 (1982).
5. Curie, P. & Laborde, A. *C. r. hebd. Séanc. Acad. Sci. Paris* 136, 673-675 (1903).
6. Ellis, C. D. & Wooster, A. *Proc. R. Soc.* A117, 109-123 (1927).
7. Cannon, C. V. & Jenks, G. H. *Rev. Sci. Instrum.* 21, 236-240 (1950).
8. Simon, S. *Nature* 135, 763 (1935).
9. Dalmazzone, J. *Rapport* CEA-R-4858 (France), 1-39 (1977).
10. Moseley, S. H., Mather, J. C. & McCammon, D. *J. appl. Phys.* 56(5), 1257-1262 (1984).
11. McCammon, D., Moseley, S. H., Mather, J. C. & Mushotzky, R. F. *J. appl. Phys.* 56(5), 1263-1266 (1984).
12. Fiorini, E. & Niinikoski, T. *Nucl. Instrum. Meth.* 224, 83-88 (1984).
13. Low, P. J. *J. opt. Soc. Am.* 51, 1300-1304 (1961).
14. Coron, N., Dambier, G. & Leblanc, J. in *Infrared Detector Techniques for Space Research* (eds Manno, V. & Ring, J.) 121-131 (Reidel, Dordrecht, 1972).
15. Clegg, P. E., Ade, P. A. R. & Rowan-Robinson, M. *Nature* 249, 530-532 (1974).
16. Roellig, T. P. L. & Houck, J. R. *Int. J. Infrared mm Waves* 4, 299-309 (1983).
17. Lauge, A. E., Kreysa, E., McBride, S. E. & Richards, P. L. *Int. J. Infrared mm waves* 4, 689-706 (1983).
18. Mather, J. C. *Appl. Optics* 23, 584-588 (1984).
19. Bassi, D., Dondi, M. G., Tommasini, F., Torello, F. & Valbusa, U. *Phys. Rev.* A13, 584-594 (1976).
20. Gough, T. E., Miller, R. E. & Scoles, G. *Appl. Phys. Lett.* 30, 338-340 (1977).
21. Houck, J. R. & Briotta, D. A. Jr *Infrared Phys.* 22, 215-219 (1982).
22. Dambier, G., Leblanc, J., Moalic, J. P., Coron, N. & Liuant, J. *French Patent* No. 2.410.211 (77 36217)(Nov. 1977).
23. Stefanovitch, D. *Rev. Sci. Instrum.* 47, 239-240 (1976).

An apparently first-order transition between two amorphous phases of ice induced by pressure

O. Mishima, L. D. Calvert & E. Whalley

Division of Chemistry,
National Research Council,
Ottawa, Canada K1A OR6

We recently reported[1] a transition from ice Ih to a high-density amorphous phase at 10 kbar, 77 K. Here we report that low-density amorphous ice (density 0.94 g cm^{-3}) compressed at 77 K transforms to high-density amorphous ice (1.19 g cm^{-3} at zero pressure) at a sharp transition at 6±0.5 kbar. The transition is at least as sharp as the previously reported[1] transition and strongly resembles a first-order transition in its sharpness and large volume change. It appears to be the first example of an apparently first-order transition between amorphous solids and has implications not only for our understanding of the behaviour of condensed matter, but also for theories of planetary interiors.

Ice Ih at 77 K, when compressed to its extrapolated melting pressure of 10 kbar, transforms very readily (in view of the temperature) to an amorphous solid of density 1.31± ~0.02 g cm^{-3} at 10 kbar and 1.17± ~0.02 g cm^{-3} at zero pressure[1]. The transformation seems to be of a new kind, in which a solid 'melts', at an apparently first-order transition well within the glass region of the liquid, to produce an amorphous phase that resembles the glass at the temperature and pressure of the experiment. When heated at zero pressure, the new phase transforms at ~117 K to an amorphous phase whose X-ray diffraction pattern resembles that of the amorphous ice made by condensing the vapour on a cold surface[2,3]. We have since determined the density of this phase, by weighing in liquid nitrogen, to be 0.94± ~0.02 g cm^{-3}.

The low-density amorphous ice would no doubt become less stable than the high-density amorphous ice it was made from, if it were put under high enough pressure. Eventually, it might transform to a high-density amorphous form resembling that made by squeezing ice I, perhaps at an apparently first-order transition resembling that of ice I[1] and, if so, its density would increase by ~23%. Such an apparently first-order transformation of one amorphous phase to another with a large increase in density seems not to have been reported, although gradual

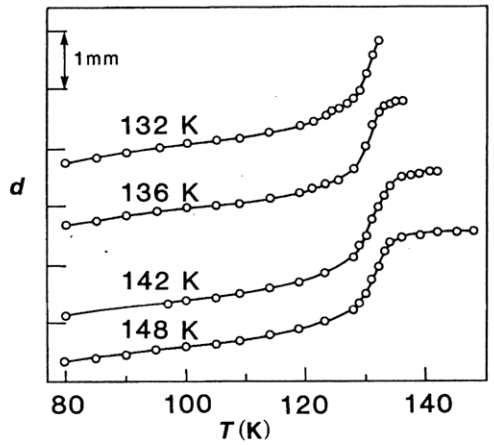

Fig. 1 The evolution of low-density amorphous ice from the high-density amorph. High-density amorphous ice was prepared by compressing about 1.0–1.2 cm^3 of water in an indium cup at 77 K to ~16 kbar in a steel vessel of 12.5 mm inside diameter, 50-mm outside diameter and 75-mm length, using a hydraulic press[1], and the pressure was reduced to a nominal pressure of 100 bar. The samples were heated in the pressure vessel at the rate of ~1 K min^{-1} to 132, 136, 142 and 148 K, as marked on the curves, and then quenched by immersing in liquid nitrogen. The temperature was measured by a thermocouple attached to the pressurizing piston and the sample may be slightly cooler than the thermocouple. The displacement of the piston is plotted against temperature in the figure.

densifications of amorphous phases of up to 20%, when squeezed to ~100 kbar with or without shearing, have been reported[4–9]. The compression of amorphous ice, reported here, should therefore be very interesting.

Four samples of high-density amorphous ice were made by compressing ice I at 77 K in an indium cup inside a steel pressure vessel[1] to ~16 kbar. The pressure was then reduced to 0.1 kbar and the pressure vessel and its contents were heated to 132, 136, 142 or 148 K at a rate of ~1 K min^{-1} to transform the high-density amorphous ice into the low-density amorph; the increase in volume was followed by the displacement of the piston. The sample was then cooled rapidly to 77 K.

The piston displacement during each of the four runs is plotted against the temperature in Fig. 1. The displacement changes rapidly with temperature above ~128 K because the high-density amorphous ice is transforming to low-density. The samples heated to 136, 142 and 148 K, which contained significantly different amounts of water, seem to have been completely transformed to the low-density form in the time of the experiment, but the sample heated to 132 K was incompletely transformed.

The low-density amorphous ice was then compressed and decompressed at 77 K in the same apparatus. The displacement of the piston during the compressions and decompressions is plotted in Fig. 2, where it is compared with the compression of a similar amount of ice Ih[1] (lowest curve). All the low-density amorphous samples compressed elastically until the sample pressure, corrected for friction, reached 6 ± ~0.5 kbar (the uncertainty is mainly due to friction in the apparatus), when a rather sudden (in view of the low temperature) transition started and the volume decreased by 4.0 ± ~0.3 cm^3 mol^{-1} or ~22%. Half of the compression occurred in a pressure range of ~0.5 kbar and the transformation seemed complete at 8–9 kbar. The transformation did not reverse when the pressure was decreased and the sample expanded only elastically. The samples that had been prepared by heating to 142 and 148 K transformed at the 6-kbar transition, but underwent another inelastic compression starting at ~10 kbar. No doubt some ice Ih[1] or Ic was formed when the samples were heated; when the samples were compressed, the ice transformed to high-density amorphous ice at 10 kbar[1], as is the case for ice Ih.

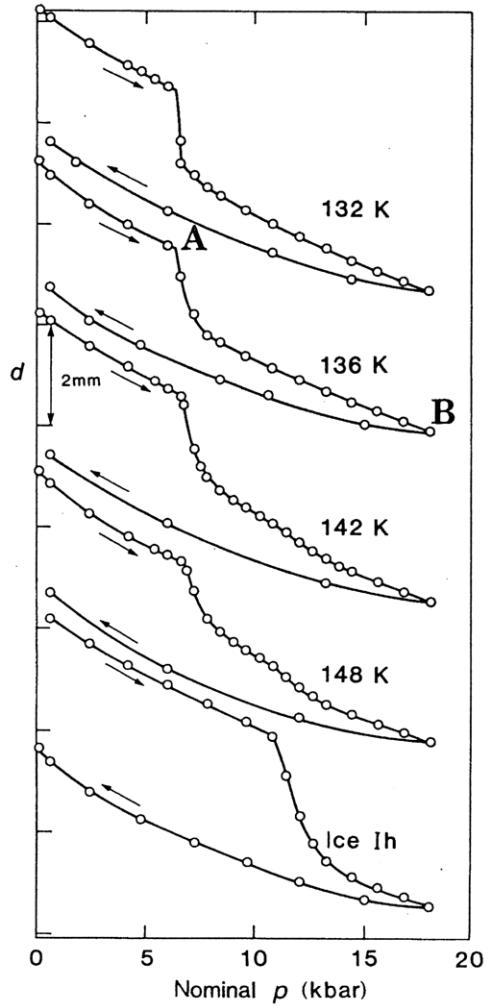

Fig. 2 Compression at 77 K to 16 kbar and decompression of the four samples of low-density amorphous ice. They were made as described in Fig. 1 legend. The arrows show the direction of the pressure changes, and the samples are identified by the temperature at which they were formed. The compression of ice Ih at 77 K is plotted as the lowest curve for comparison.

The density of the high-density phase at 6 kbar was estimated from the piston displacement to be 1.26 ± ~0.02 g cm^{-3}, and 1.19 ± ~0.02 g cm^{-3} at zero pressure. The zero-pressure density is equal, within the experimental uncertainty, to that (1.17 g cm^{-3}) of the amorph made by transforming ice Ih at 77 K and zero pressure.

Samples were recovered from the conditions represented by points A and B of the 136-K run in Fig. 2 and microphotometer traces of their X-ray diffraction patterns are reproduced in Fig. 3. The pattern of sample A is, within the experimental uncertainty, the same as that of low-density amorphous ice[1] and the pattern of sample B is the same as that of the high-density amorphous ice made by compressing ice Ih at 77 K to 10 kbar[1]. There is no doubt that the phase produced by the 6-kbar transition of low-density amorphous ice at 77 K is another amorphous phase and is similar to the high-density amorphous ice made by transforming ice I at 10 kbar[1].

The seemingly almost discontinuous transition from low-density to high-density amorphous ice with a decrease of volume of ~22% resembles, in its sharpness, the 'melting' of ice I at 77 K and 10 kbar to the 'liquid' in the glass region[1]. It seems that the low-density amorphous ice becomes unstable, relative to the high-density amorphous phase, perhaps at its surface, where ice I seems to become unstable[1], and undergoes a new kind of apparently discontinuous transition between two amorphous phases which at least approximates first-order behaviour. The phase that is produced strongly resembles the amorphous

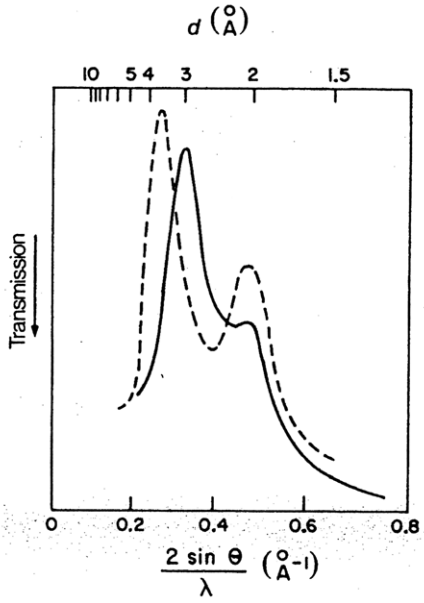

Fig. 3 Representative microphotometer tracings as a function of $(2 \sin \theta)/\lambda$, where 2θ is the scattering angle and λ, the wavelength of the X rays, of diffraction patterns of homogeneous samples of low-density amorphous ice (dashed line) and of the high-density amorphous ice (solid line) taken in a flat-plate X-ray camera. The temperature was controlled to ±5 K by flowing nitrogen gas and was measured by a thermocouple placed near the specimen. Photographs were taken at ~95 K using zirconium-filtered molybdenum radiation.

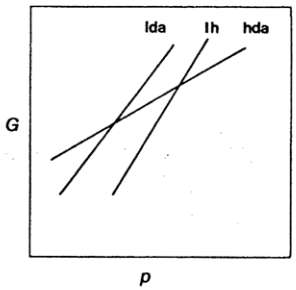

Fig. 4 Schematic graph of the Gibbs function G against the pressure p for ice Ih and low-density (lda) and high-density (hda) amorphous ice.

ice made by transforming ice I, and the transition seems to be a new way of making amorphous phases.

The pressure of the amorph–amorph transition is 4 kbar lower than that of the transition of ice I to amorphous ice at the same temperature. The difference in the transition pressures is readily understood if both transitions are considered as first-order, as they seem to be to a good approximation because they are so sharp and occur with a large volume change. The specific Gibbs functions of ice Ih, low-density amorphous ice and high-density amorphous ice are plotted schematically against the pressure in Fig. 4. From the equation $dG/dp = V$, it is readily shown that the Gibbs-function difference for two phases at zero pressure which are in equilibrium at pressure p_e is, to first order and neglecting the compressibility difference of the two phases, $\Delta G(p=0) = -\Delta V(p=0)p_e$, where ΔV is the volume difference of the two phases. The value of p_e for transformation to the high-density amorphous phase will be tentatively assumed to be the experimental transformation pressure. From the transformation pressure of ice Ih to high-density amorph[1] (hda) and of low-density (lda) to high-density amorph, and from the specific volumes of the phases at zero pressure, the Gibbs-function differences at zero pressure are $\Delta^{hda}_{Ih}G(p=0) = 4.1 \pm \sim 0.3$ and $\Delta^{hda}_{lda}G(p=0) = 2.5 \pm \sim 0.3$ kJ mol^{-1}, so that $\Delta^{lda}_{Ih}G(p=0) = 1.6 \pm \sim 0.3$ kJ mol^{-1}.

A similar transformation ought to occur in other four-coordinated amorphous solids, such as amorphous silicon and germanium. These materials crystallize when compressed at room temperature[10,11], but may form high-density amorphous phases if compressed at low temperature.

The ultimate phase of ice, as far as is known, is ice VII or VIII, both based on a body-centred-cubic arrangement of the oxygen atoms, and the corresponding phase having centrosymmetric hydrogen bonds, known as ice X[12,13]. The density of ice VIII when recovered at zero pressure and 77 K is 1.46 g cm^{-3} (ref. 14), about 25% denser than our high-density amorphous ice. The high-density amorphous ice may, therefore, undergo yet another transformation, either gradually or suddenly, if it is subjected to high enough pressures. We are presently testing this suggestion.

Finally, this amorphous–amorphous transition may be important in the planets. The ice formed in space from gaseous molecules is very probably amorphous[15] and if it agglomerates to form a planet, it will transform to the high-density amorph if the planet becomes large enough, that is, having a radius of the magnitude of 2 Mm.

We thank the National Research Council of Canada for a Research Associateship for O.M. (1983–85). This work is NRC No. 24042.

Received 26 November; accepted 20 December 1984.

1. Mishima, O., Calvert, L. D. & Whalley, E. *Nature* **310**, 393–395 (1984).
2. Bondot, P. *C. r. hebd. Séanc. Acad. Sci., Paris* **B265**, 316–318 (1967); **B268**, 933–936 (1969).
3. Venkatesh, C. C., Rice, S. A. & Bates, J. B. *J. chem. Phys.* **63**, 1065–1071 (1975).
4. Bridgman, P. W. & Simon, I. *J. appl. Phys.* **24**, 405–413 (1953).
5. Bridgman, P. W. *Proc. Am. Acad. Arts Sci.* **84**, 111–129 (1955).
6. Cohen, H. M. & Roy, R. *J. Am. ceram. Soc.* **44**, 523–524 (1961).
7. Christiansen, E. B., Kistler, S. S. & Gogarty, W. B. *J. Am. ceram. Soc.* **45**, 172–177 (1962).
8. Cohen, H. M. & Roy, R. *Phys. Chem. Glasses* **6**, 149–161 (1965).
9. Poch, W. *Phys. Chem. Glasses* **8**, 129–131 (1967).
10. Shimomura, O. *et al. Phil. Mag.* **29**, 547–558 (1974).
11. Minomura, S., Shimomura, O., Asaumi, K., Oyanagi, H. & Takemura, K. *Proc. 7th Int. Conf. Amorphous Liquid Semiconductors* (ed. Spear, W. E.) 53–57 (Centre for Industrial Consultancy and Liaison, University of Edinburgh, 1977).
12. Hirsch K. R. & Holzapfel, W. B. *Phys. Lett.* **101A**, 142–144 (1984).
13. Polian, A. & Grimsditch, M. S. *Phys. Rev. Lett.* **52**, 1312–1314 (1984).
14. Bertie, J. E., Calvert, L. D. & Whalley, E. *Can. J. Chem.* **42**, 1373–1378 (1964).
15. Klinger, J. *J. phys. Chem.* **87**, 4209–4214 (1983).

Al^{3+} coordination changes in liquid aluminosilicates under pressure

Eiji Ohtani*†, Francis Taulelle‡ & C. Austen Angell§

* Research School of Earth Sciences, Australian National University, Canberra, ACT, Australia
‡ Laboratoire de Physique Thermique, ESPCI, 10 Rue Vauquelin, 75005 Paris, France

Geochemists often debate the conditions in which Al^{3+} may become 6-coordinated in molten silicates and how such liquid structures are related to those of coexisting crystal phases[1–4]. To date no experimental evidence for the occurrence of Al^{3+} in this coordination state has been presented and computer simulation studies have suggested that pressures exceeding 100 kbar may be required for the 4 → 6 conversion[5,6]. To examine this question in the laboratory, we have taken advantage of the ability of the glass transition to freeze the structural equilibrium of a high-pressure melt and preserve it for subsequent examination in ambient conditions. Glasses of albite composition have been prepared by quenching melts under pressures of 0–80 kbar (0–8 GPa). The Al^{3+} coordination has been determined by ^{27}Al solid-state NMR spectrometry. We find that the 4-coordinated state is retained to pressures well beyond 30 kbar. A new peak at −16 p.p.m. relative to $Al(H_2O)^{3+}_6$, which we associate with octahedral Al^{3+} appears weakly at 60 kbar and becomes a prominent feature of the spectrum at 80 kbar.

† Present address: Department of Earth Sciences, Faculty of Science, Ehime University, Matsuyama, 790 Japan.
§ Permanent address: Department of Chemistry, Purdue University, West Lafayette, Indiana 47907, USA.